

Accepted Manuscript

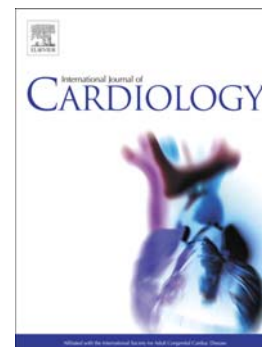
Enhanced diagnostic utility achieved by myocardial blood analysis: A meta-analysis of noninvasive cardiac imaging in the detection of functional coronary artery disease

Neng Dai, Xianlin Zhang, Yi Zhang, Lei Hou, WeiMing Li, Bing Fan, TianSong Zhang, YaWei Xu

PII: S0167-5273(16)31391-2
DOI: doi: [10.1016/j.ijcard.2016.07.031](https://doi.org/10.1016/j.ijcard.2016.07.031)
Reference: IJCA 22997

To appear in: *International Journal of Cardiology*

Received date: 16 May 2016
Accepted date: 4 July 2016



Please cite this article as: Dai Neng, Zhang Xianlin, Zhang Yi, Hou Lei, Li WeiMing, Fan Bing, Zhang TianSong, Xu YaWei, Enhanced diagnostic utility achieved by myocardial blood analysis: A meta-analysis of noninvasive cardiac imaging in the detection of functional coronary artery disease, *International Journal of Cardiology* (2016), doi: [10.1016/j.ijcard.2016.07.031](https://doi.org/10.1016/j.ijcard.2016.07.031)

This is a PDF file of an unedited manuscript that has been accepted for publication. As a service to our customers we are providing this early version of the manuscript. The manuscript will undergo copyediting, typesetting, and review of the resulting proof before it is published in its final form. Please note that during the production process errors may be discovered which could affect the content, and all legal disclaimers that apply to the journal pertain.

**Enhanced diagnostic utility achieved by myocardial blood analysis: A
meta-analysis of noninvasive cardiac imaging in the detection of functional
coronary artery disease**

by

Neng Dai^{a,b} *M.D.; Xianlin Zhang^{a*}, M.D., Ph.D; Yi Zhang^a M.D., Ph.D.
Lei Hou^a M.D., Ph.D.; WeiMing Li^a M.D.;
Bing Fan^c M.D.; TianSong Zhang^d, M.D.; YaWei Xu^a M.D., Ph.D.

from

^aCardiology Department, Tenth People's Hospital of Tongji University, Shanghai,
China;

^b Center for Systems Biology, Massachusetts General Hospital, Harvard medical
School, Boston, MA, USA;

^cCardiology Department, ZhongShan Hospital of Fudan University, Shanghai, China;

^d Department of TCM, Jing'An District Centre Hospital, Shanghai, China

*Neng Dai and Xianlin Zhang Contribute equally to this article.

Correspondence to:

Dr. YaWei Xu

Cardiology Department, Tenth People's Hospital of Tongji University
No.301 Middle Yanchang Road, Shanghai, China, 200072

Tel: +8602166300588

Fax: +8602166300588

E-mail: xuyaweish@aliyun.com

OR

Dr. Bing Fan

Cardiology Department, ZhongShan Hospital of Fudan University
180 Fenglin Road, Shanghai, China

Tel: +8613901996108

Fax: +86021-64041990

E-mail: fanbingzs@126.com

OR

Dr. TianSong Zhang

Department of TCM, Jing'An District Centre Hospital
259 Xikang Road, Shanghai, China, 200040

Tel: +8602162794791

Fax: +8602162036989

Email: ztsdoctor@126.com

Abstract:**Aim:**

The aim of this study is to determine the diagnostic utility of 6 cardiac imaging modalities using fractional flow reserve (FFR) as the reference standard.

Methods:

Studies reporting diagnostic performance of computed tomographic perfusion imaging (CTP), fractional flow reserve derived from computed tomography (FFR_{CT}), cardiac magnetic resonance (CMR), positron emission tomography (PET), single-photon emission computed tomography (SPECT) and dobutamine stress echocardiography (DSE) for diagnosis of ischemia-causing lesions were included.

Results:

On vessel-based and patient-based analyses, CMR, PET, CTP and FFR_{CT} exhibited comparable sensitivity (per-vessel: 87% vs. 86% vs. 89% vs. 86%; per-patient: 88% vs. 90% vs. 88% vs. 90%, $P>0.05$) and specificity (per-vessel: 89% vs. 88% vs. 89% vs. 83%; per-patient: 84% vs. 84% vs. 87% vs. 75%, $P>0.05$); whereas SPECT yielded significantly lower sensitivity (Per-vessel: 72%; Per-patient: 78%, $P<0.05$) and specificity (Per-vessel: 79%; Per-patient: 79%, $P<0.05$) and DES yielded significantly lower sensitivity (Per-vessel: 62%, Per-patient: 69%, $P<0.05$). On the other hand, within same imaging modality, myocardial blood flow (MBF) derived by CTP had a higher sensitivity (90% vs. 80%, $P=0.048$) but lower specificity (77% vs. 93%, $P=0.02$) than that of perfusion defect (PD). Moreover, MBF derived by CMR had a lower specificity than that of PD (60% vs. 93%, $P=0.02$), while coronary flow reserve (CRF) derived by PET had a lower specificity than that of MBF (81% vs. 89%, $P=0.005$).

Conclusion:

CMR, PET, CTP and FFR_{CT} expressed similar and high accuracy in detecting functional CAD, whereas different analysis methods for each imaging modality may vary their diagnostic utility.

Key words:

Cardiac imaging; coronary artery disease; noninvasive imaging; fractional flow reserve

Introduction

Coronary artery disease (CAD) is the leading cause of death and disability in developed countries. Although CAD mortality rates have declined over the past four decades, it remains the cause of death for approximately one-third^{1,2} of individuals over 35.

Choosing the right noninvasive imaging modalities for evaluating the presence and severity of CAD can be challenging but remains critically important for diagnosis and management. Presently, imaging tests available for this purpose include: nuclear myocardial perfusion imaging (MPI) (single-photon emission computed tomography [SPECT] and positron emission tomography [PET]), dobutamine stress echocardiography (DSE), and cardiac magnetic resonance imaging (CMR); in addition, some new examinations such as FFR_{CT} (which was the fractional flow reserve [FFR] derived in coronary models reconstructed by Computed Tomographic Angiogram [CTA]) and computed tomographic perfusion imaging (CTP, which was myocardial perfusion imaging initiated after administration of adenosine by CT scan) are currently being investigated as novel alternatives.

Meta-analyses³⁻⁶ have previously evaluated the individual diagnostic performance of various cardiac imaging approaches for the detection of CAD as defined by FFR. However, only a very limited number of studies have specifically compared the diagnostic utility of imaging tests against each other and/or were designed in such a way to preclude an unbiased evaluation⁷⁻⁹, in addition, their conclusions have not always been concordant.

We conducted a meta-analysis to evaluate the diagnostic performances of 6 cardiac imaging modalities, including the traditional modalities (i.e., SPECT, CMR, PET and DSE) and emerging approaches (CTP and FFR_{CT}) from a functional

viewpoint using FFR as the reference standard. We also compared the diagnostic utility of each test against each other and evaluated factors that may affect the diagnostic performance of each imaging approach.

Methods

We searched PubMed and the Cochrane Central Register of Controlled Trials on June 20th 2015 to identify all trials about CTP, FFR_{CT}, CMR, PET, SPECT, and DSE published up to June 2015. Keywords were “*computed tomographic perfusion*”, “*FFR CT*”, “*computed tomography*”, “*single-photon emission computed tomography*”, “*magnetic resonance imaging*”, “*positron emission tomography*”, “*myocardial perfusion*”, “*stress echocardiography*”, and “*fractional flow reserve*”. Additionally, our search was limited to “humans” and “English”.

Two authors (N.D., Y.Z.) identified relevant original articles and extracted the data independently, while a third author (Y.-W.X.) evaluated the results. Any disagreement was resolved by discussion until a consensus was reached.

Inclusion criteria for selected studies were: (1) assessment of CTP, FFR_{CT}, DSE, SPECT, PET, or CMR for diagnosis of ischemia-causing lesions according to invasive FFR; (2) absolute numbers of true positive (TP), false positive (FP), true negative (TN), and false negative (FN) results, or if these data were derivable from the presented results.

Extracted information from the selected studies included: study characteristics (study name, authors, publication year, study sites, study period and number of participants and vessels), participants’ characteristics (mean age or age range, gender), study inclusion and exclusion criteria, reported or derived absolute numbers of true positive, false positive, true negative, and false negative results of these noninvasive cardiac imaging in CAD.

Several studies used >1 cutoff value for CAD and, as a consequence, reported >1 pair of sensitivity and specificity. To improve the comparability of study results in the analysis of overall diagnostic performance, we selected a cutoff value of <0.80 whenever possible. However, if data were not reported for a cutoff value of <0.80 , we selected the cutoff value that was available (e.g., <0.75). In addition, subgroup analysis was applied regarding the cutoff value to assess whether the primary results were affected. If a study presented multiple sensitivity and specificity estimates for the selected cutoff value due to different study protocols (e.g., exercise versus pharmacological stress) or the different examination assessment indexes in the same imaging test (e.g., summed stress score versus summed difference score in SPECT), the data of the protocol with the highest estimates was extracted; while each group was considered for the subgroup analysis. In cases where >1 diagnostic technique was evaluated within a single publication (e.g., SPECT versus CMR), each modality was considered separately. The diagnostic performance of these imaging modalities in intermediate stenosis (which was defined as a 50-70% stenosis on CT or coronary angiogram) was also retrieved when data were available.

Quality assessment was performed using guidelines published by the standards for reporting diagnostic accuracy (STARD) initiative¹⁰ (maximum score 25), and the revised quality assessment for studies of diagnostic accuracy (QUADAS-2) tool¹¹ (see Appendices: Online Tables 1 and 2).

In the included studies^{Online references 9-21}, CTP imaging was assessed by visual or quantitative analysis. For visual analysis, perfusion defect was determined as recommended in the standard American Heart Association 17-segment model^{12, Online reference¹⁵}; for quantitative analysis, myocardial blood flow (MBF, Time-attenuation curves were calculated for the left ventricular myocardium and the left ventricular

cavity. A linear fit was calculated from the foot-point to the peak of the time-attenuation curves, the regional MBF was determined by using the following equation: $US_{MC}/PE_{LVC} \cdot \kappa$, where US_{MC} is the upslope in the myocardium, PE_{LVC} is the peak enhancement in the left ventricular cavity, and κ is a correction factor of 1.5 mL/g/min used to calculate the MBF^{Online reference 13)} or transmural perfusion ratio (TPR, which was calculated as the ratio of the segment-specific subendocardial attenuation density to the mean attenuation density of the entire subepicardial layer of any given short-axis slice. The segment with the lowest transmural perfusion ratio value was chosen to represent perfusion for each major vessel) were assessed.

For FFR_{CT} analysis, the included studies applied mainly two different patient-specific models to compute coronary fractional flow reserve: model developed by Siemens^{13, Online reference 6)} (Siemens cFFR, Version 1.4; Siemens Healthcare, currently not commercially available) and model developed by HeartFlow^{14, Online reference 1-3)}.

For CMR imaging analysis, perfusion defect, Myocardial perfusion reserve index (MPRI) and myocardial blood flow (MBF) are used in different studies, perfusion defect was defined as hypo-enhancement lasting more than three consecutive images after the arrival of the contrast agent in the left ventricular cavity; endocardial and epicardial borders were outlined and a region of interest placed in the LV cavity, MPRI was calculated by dividing the hyperemic myocardial blood flow estimate flow by resting flow^{Online reference 31)}. MBF was calculated by signal intensity curve.

For PET imaging analysis, besides MBF as that used in CMR and CTP analysis, coronary flow reserve (CFR), which was defined as the ratio of hyperaemic and baseline MBF, was also derived^{Online reference 41-44)}.

For SPECT imaging analysis, Perfusion SPECT images were scored as

previously described¹⁵. The stress and rest images were divided according to the 17 standardized myocardial segments and the regional tracer uptake in each segment was semi-quantitatively determined. The sum of the stress scores of all segments, the summed stress score (SSS), and the sum of the rest scores of all segments, the summed rest score (SRS), were determined. A summed difference score (SDS) was calculated as the difference of SSS and SRS. The regional perfusion score was then calculated as the sum of individual segmental scores for each vessel territory.

The standard LV 16-segment model as recommended by the American Society of Echocardiography was applied for DSE analysis. Accordingly, segments 1, 2, 7, 8, 12, 13–16 were defined as left anterior descending (LAD) artery perfusion territory, segments 3, 4, 9, 10 as right circumflex (RCX) artery perfusion territory, and segments 5, 6, 11 as right coronary artery (RCA) perfusion territory.¹⁰ Segments were evaluated regarding wall thickening and radial movement of the LV endocardium, which was classified semiquantitatively on a four-point scale as normo-, hypo-, a- or dyskinetic ^{Online reference 66-70}.

Our primary outcomes are diagnostic performances of CTP, FFR_{CT}, CMR, PET, SPECT, DSE and their relationships. The comparisons of sensitivities and specificities of these techniques, and their diagnostic performances in sub-groups (such as different imaging evaluation methods in each imaging modality are the secondary outcomes) were evaluated.

The pooled sensitivity, specificity, positive likelihood ratio (PLR), negative likelihood ratio (NLR), diagnostic odds ratio (DOR, which is computed as the ratio of positive to negative likelihood ratios and provided an estimate of how much greater the odds of having the disease are for the people with a positive test result than for the people with a negative test result), and summary Receiver Operating Characteristic

(SROC) for each imaging modality were conducted by bivariate analysis¹⁶⁻¹⁹. In addition, the pooled sensitivity, specificity and area under SROC of the six imaging modalities were compared using the bivariate approach by Stata13.0 “midas9” command¹⁷. A perfect test has an area under the curve (AUC, representing an analytical summary of test performance and displays the trade-off between sensitivity and specificity) close to 1; poor tests have AUCs close to 0.5. SAS software version 9.2 (SAS Institute, Cary, North Carolina, USA) was applied for the comparisons among different cardiac imaging modalities. R3.20 with “mada” was used to compare the fitted SROCs of different imaging tests. Pooled estimates were calculated for subgroups of studies that were defined according to specific study characteristics. The RDORs with 95% confidence interval (CI) were calculated to quantify the differences in pooled odds ratios between subgroups. In addition to the comparison of subgroups within a single imaging modality, the pooled DORs of the subgroups were also compared between the different imaging modalities. Publication bias was examined using Deeks' test²⁰ (See Appendices).

Results

Our initial literature search identified 530 published articles. Screening of titles and abstracts showed that 430 of these articles did not meet our inclusion criteria in regards to their topics or article types. Full article of the remaining 99 papers were retrieved for further review, 25 were excluded for reasons listed in Fig.1. In total, 74[8 FFR_{CT} (n=850), 21CMR (n=1,320), 20SPECT (n=1,517), 5PET (n=675), 12CTP (n=644), 8 DSE (n=405), among which one study reported diagnostic performance of both CTP and CMR, one reported diagnostic performance of both SPECT and CMR and another reported both reported diagnostic performance of both SPECT and DSE] studies^{Online References 1-71} were included for final analysis. The characteristics of the

included studies are shown in Table 1.

Pooled estimates of sensitivity, specificity, PLR, NLR, DOR and area under SROC (AUROC) of the 6 imaging modalities on both patient and coronary artery territory levels are summarized in Table 2. As shown in Figure.2, when comparing these imaging modalities with each other on per-patient analysis, the sensitivities for CMR (88% vs. 69%, $P=0.009$), FFR_{CT} (90% vs. 69%, $P=0.006$), CTP (88% vs. 69%, $P=0.029$) and PET (90% vs. 69%, $P=0.014$) were significantly higher than that of DSE; in addition, the sensitivity of CMR was found to be higher than that of SPECT (88% vs. 78%, $P=0.039$) and the specificity of SPECT was significantly higher than that of FFR_{CT}; while on per-vessel analysis, the sensitivities of CMR (87% vs. 62%, $P=0.020$) and CTP (89% vs. 62%, $P=0.038$) were significantly higher than that of DSE, the sensitivities of CMR (87% vs. 72%, $P=0.0002$), FFR_{CT} (86% vs. 72%, $P<0.0001$), CTP (89% vs. 72%, $P=0.002$) and PET (86% vs. 72%, $P=0.015$) were significantly higher than that of SPECT; while the specificities of CMR (89% vs. 79%, $P=0.023$), FFR_{CT} (83% vs. 79%, $P<0.0001$) and CTP (89% vs. 79%, $P<0.025$) were significantly higher than that of SPECT. (Online Tables 3 and 4).

The overall diagnostic accuracy of CMR, CTP, FFR_{CT}, PET, SPECT, and DSE to detect functionally significant CAD on per-patient and per-vessel analysis were summarized in Table 2 and Figure 3. On per-vessel analysis, the diagnostic accuracy of CMR, FFR_{CT}, CTP and PET are significantly higher than that of SPECT (0.94, 0.89, 0.94 and 0.92 vs. 0.83, $P<0.05$) and DSE (0.94, 0.89, 0.94 and 0.92 vs. 0.86, $P<0.05$); while on per-patient analysis, CMR, FFR_{CT}, CTP and PET had a significantly higher accuracy than DSE (0.91, 0.90, 0.94 and 0.92 vs. 0.78, $P<0.05$), CMR, CTP and PET had a significantly higher accuracy than SPECT (0.91, 0.94 and 0.92 vs. 0.85, $P<0.05$).

Diagnostic performances of FFR_{CT} , CMR, CTP, SPECT and DSE in patients with intermediate stenosis were displayed in Appendix (Online Figure 1), diagnostic accuracy of FFR_{CT} , CMR and CTP remained unchanged, while DSE had a significantly higher sensitivity but lower specificity.

On per-vessel analysis, there were 10 studies reported diagnostic performance of PD, 3 studies reported diagnostic performance of MBF, and 4 studies reported diagnostic performance of MPRI. The pooled sensitivity and specificity for each of the analysis index were listed in Table 3. Comparison revealed that PD had a similar sensitivity (83% vs. 83%, $P=0.633$) but significantly higher specificity (90% vs. 60%, $P=0.022$) than MBF. While MBF had a similar sensitivity (83% vs. 92%, $P=0.107$) and specificity (60% vs. 84%, $P=0.599$) as compared to MPRI; PD also had a similar sensitivity (83% vs. 92%, $P=0.115$) and specificity (90% vs. 84%, $P=0.063$) as compared to MPRI (Table 4, Figure 4).

On per-vessel analysis, 5 studies reported diagnostic performance of PD and 4 studies reported diagnostic performance of MBF. Our results revealed that PD had a significantly lower sensitivity (80% vs. 90%, $P=0.048$) but higher specificity (93% vs. 77%, $P=0.020$) when compared with MBF (Tables 3, 4, Figure 4).

On per-vessel analysis, 4 studies reported diagnostic performance of CRF, 6 studies reported diagnostic performance of MBF, on per-patient analysis, diagnostic performance of CRF was reported in 3 studies and diagnostic performance of MBF was reported in 5 studies. Our results revealed that CFR had a significantly lower specificity on both per-vessel (81% vs. 89%, $P=0.005$) and per-patient (75% vs. 87%, $P=0.008$) analysis. Their sensitivities were similar on both per-vessel (78% vs. 88%, $P=0.143$) and per-patient (84% vs. 91% $P=0.307$) analysis (Tables 3, 4, Figure 4).

Comparison of other imaging indexes or analysis methods for FFR_{CT} and SPECT

were listed in Appendices (Online Tables 5, 6)

Subgroup analyses were performed to identify sources of variation between study results (Online Tables 7-10) and to evaluate whether differences in distribution of study characteristics between modalities affect the results. The analyses revealed no significant effect of test and study characteristics on the diagnostic performance of the 6 modalities, except for a lower pooled DOR of CMR studies in patients with suspected CAD when compared to those with suspected or known CAD; while the CTP in patients with suspected CAD reported a higher pooled DOR than in those with suspected or known CAD. The SPECT studies using attenuation correction demonstrated a higher sensitivity and specificity in comparison to studies without attenuation correction, thus a higher pooled DORs for SPECT studies with and without attenuation correction.

Discussion

In this study, we have compared for the first time, to our knowledge, the diagnostic accuracy of the CMR, CTP, FFR_{CT}, PET, SPECT and DSE with invasive functional standard, FFR, as reference. Also, we determined that the imaging evaluation method for each imaging may affect their diagnostic accuracy.

Our analysis revealed that on vessel-based analysis, CMR has a similar AUC as PET and CTP while significantly higher AUC than that of SPECT; on per-patient level, the diagnostic performance FFR_{CT} was similar with those of CMR, CTP and PET, but significantly higher than that of DSE. Among these imaging modalities, CMR, CTP and PET all had high sensitivity and specificity; FFR_{CT} had high sensitivity but low specificity on patient based analysis. MBF derived by CTP had a higher sensitivity but lower specificity (77% vs. 93%, $P=0.020$) than that of perfusion

defect on vessel-based analyses, leading to a similar diagnostic accuracy (0.91 vs. 0.95, $P=NS$). MBF derived by PET had a higher AUC than that of CFR (coronary flow reserve) on both per-vessel (0.93 vs. 0.86, $P<0.05$) and per-patient (0.93 vs. 0.88, $P<0.05$) analyses.

As conventional cardiac imaging, diagnostic performances of CMR, PET and SPECT have been well validated. Several studies had revealed that diagnostic performance of CMR was superior to SPECT^{21, 22}. In CMR, reversible ischemia is visually assessed as a reversible low-signal defect in the absence of delayed enhancement and attenuation artifacts are not the limitation as those in nuclear imaging. A recent meta-analysis confirmed a high sensitivity (89%) and moderate specificity (80%) for the diagnosis of significant CAD in a population with a high prevalence of CAD of 57%²³. In addition, CMR also consistently detected more subendocardial defects than SPECT or PET imaging. Nearly half of the segments with subendocardial infarcts were missed on SPECT²⁴ and PET²⁵. For CMR, we found that the AUC of perfusion defect is higher than those of MBF and MPRI on per-patient analysis, which is out of expect that a semi-quantitative index has a higher overall accuracy than quantitative index, but a similar results can be observed in study by Lockie et al^{Online reference 31}. They observed that AUC for visual perfusion is 0.92 while AUC for myocardial perfusion reserve is 0.89.

For PET imaging analysis, our results indicated that MBF computed by PET expressed a higher diagnostic accuracy than CFR, which is in line with a previous study by Danad et al^{Online reference 42}, in which they revealed that hyperemic MBF (0.86; 95% confidence interval [CI], 0.81–0.90) had a significantly higher AUC than CFR (AUC, 0.81; 95% CI, 0.75–0.86) for the detection of obstructive CAD ($p=0.02$). In small-scaled studies, Hajjiri et al²⁶ observed a slightly higher accuracy for hyperemic

MBF, whereas Muzik et al²⁷ concluded that CFR was more accurate, although the differences were small. These observations, in combination with our currently presented data, imply that a single measurement of hyperemic MBF could suffice in PET diagnostic imaging protocols.

Prior to this analysis, few comparisons of these imaging modalities were conducted in the same population directly. Our findings were not only in accordance to these results, but also add to the present knowledge of diagnostic performance of these conventional cardiovascular imaging.

As emerging non-invasive techniques, though FFR_{CT} and CTP expressed similar diagnostic value as CMR on both patient- and vessel-based analyses, their diagnostic performances still need further verification. As we concerned before²⁸, high sensitivity is important in diagnosing CAD because missed diagnosis may lead to terrible results such as acute myocardial infarction. FFR_{CT} is a promising non-invasive cardiac imaging technique since it has a high sensitivity. However, we also observed in our analysis that FFR_{CT} has a fair specificity, which may lead to overtreatment, which is contrary to initial intention of FFR_{CT} measurement as a screening test²⁸.

CTP had a good diagnostic performance without modifying the examination protocol much and increasing the radiation exposure, which is a promising non-invasive cardiac imaging in the detection of CAD. Ho et al²⁹ compared CTP with SPECT, revealing a sensitivity of 95% and a specificity of 83% of CTP for the detection of haemodynamically relevant stenosis. George et al³⁰ investigating patients with suspected or known CAD, found a sensitivity of 100% and a specificity of 81% of CTP and they reported in their recent study³¹ that the overall performance of myocardial CTP imaging in the diagnosis of anatomic CAD (stenosis $\geq 50\%$), was higher than that of SPECT (0.78 vs. 0.69, $p=0.001$), which is in line with our findings.

In patients with intermediate lesions in coronary arteries, the assessment for the lesion is complex but important. Our results revealed that the diagnostic performances of CMR, CTP and FFR_{CT} remained unchanged but DSE, however, further studies are needed to verify our findings.

In the current analysis, FFR was used as the reference for the detection of functional significant CAD. The prognostic value of FFR is widely accepted, as FAME, FAME II, and DEFER³²⁻³⁴ all demonstrated the benefits of FFR-guided PCI in terms of event reduction (predominantly a reduction in urgent revascularization). However, FFR has never to be claimed as the diagnostic gold-standard of ischemia testing in these studies and any other studies. And FFR was itself originally validated against noninvasive stress tests³⁵, making it somewhat paradoxical and creating questionable circular arguments when being used as an endpoint for non-invasive imaging studies³⁶. Nevertheless, the initial validation study was really to determine the ischemia threshold of FFR. Once this was determined, FFR outperforms SPECT/DSE in at least three scenarios, where it is currently useful clinically. First, the pressure wire can inherently accurately measure FFR in smaller vessels supplying smaller myocardial segments than in the initial validation study, below the detection limits of either stress SPECT/DSE of high quality without artefact. Secondly, in patients susceptible to artefacts with either SPECT/DSE, the accuracy of FFR remains unaffected. Thirdly, in balanced three vessel obstructive coronary artery disease³⁷. Therefore, it is not a tautology to use FFR as a reference standard in assessing accuracy of non-invasive studies including CMR/SPECT/DSE in other patient subgroups, after initial determination of the ischemia threshold of FFR.

Finally, as with any meta-analysis, our findings need to be interpreted with an understanding of its limitations. First, not all included articles reported the absolute

numbers of TP, FP, FN and TN, and in these instances we derived from the reported sensitivity and specificity estimates, which may introduce bias; second, studies about some of the modalities are limited, and publication bias were found for CMR on vessel-based analysis (see Supplementary materials); third, for FFR_{CT}: in 3 studies, 609 patients with 1000 vessels, FFR measured in all (except for 16 total occlusions in NXT assigned FFR value of 0.5), for other modalities such as CMR, PET and SPECT, FFR was not performed in 100% of vessels; fourth, there is a grey zone of FFR cut-off value between 0.75 and 0.80, so two cut-off values of 0.75 and 0.80 were used in these studies, which would bias the results, but subgroup analyses in CMR, CTP and SPECT studies revealed that different cut-off values of FFR did not change the results significantly; fifth, the prevalence of CAD varied in different studies included, which would bias the results; sixth, different scanners and scanning protocols or parameters were used in different studies, and even for the same index, such as MBF, different centers used different models for analysis and calculation; finally, fewer data on the direct comparison among these imaging modalities are available at present, and heterogeneity was observed in these studies. Though our results remain unchanged after meta-regression and sub-group analyses.

In summary, CTP, CMR FFR_{CT}, and PET expressed high and similar accuracy in detecting functional CAD. On per-patient level, diagnostic accuracy of FFR_{CT} was significantly higher than that of DSE and diagnostic accuracy of CMR, CTP and PET were significant higher than that of SPECT; while on per-vessel level, CMR, FFR_{CT} and CTP all showed higher diagnostic accuracy than SPECT. Among these imaging modalities, CMR, CTP had PET all had high sensitivity and specificity; FFR_{CT} had high sensitivity but low specificity on patient-based analysis. MBF derived in PET has a better specificity than that of CFR. PD in CTP had s lower sensitivity but higher

specificity compared to MBF on per-vessel analysis.

Physicians can refer to our results in choosing the appropriate non-invasive examinations in consideration of not only their overall diagnostic accuracy but also their sensitivity and specificity features for patients with different likelihood of CAD.

Acknowledgments

We would love to thank Mr. YongChang Gong for help editing tables and figures.

Funding Sources

This study was funded, in part, by Country China Scholarship Council (2014OS66014261) and by the Medical Related Science and Technology Project of Shanghai Science and Technology Commission (No. 14411963100)

Disclosures

None

1. Rosamond W, Flegal K, Furie K, Go A, Greenlund K, Haase N, Hailpern SM, Ho M, Howard V, Kissela B, Kittner S, Lloyd-Jones D, McDermott M, Meigs J, Moy C, Nichol G, O'Donnell C, Roger V, Sorlie P, Steinberger J, Thom T, Wilson M, Hong Y; American Heart Association Statistics Committee and Stroke Statistics Subcommittee. Heart disease and stroke statistics--2008 update: a report from the American Heart Association Statistics Committee and Stroke Statistics Subcommittee. *Circulation*. 2008; 117:e25-146.
2. Lloyd-Jones D, Adams RJ, Brown TM, Carnethon M, Dai S, De Simone G, Ferguson TB, Ford E, Furie K, Gillespie C, Go A, Greenlund K, Haase N, Hailpern S, Ho PM, Howard V, Kissela B, Kittner S, Lackland D, Lisabeth L, Marelli A, McDermott MM, Meigs J, Mozaffarian D, Mussolino M, Nichol G, Roger VL, Rosamond W, Sacco R, Sorlie P, Stafford R, Thom T, Wasserthiel-Smoller S, Wong ND, Wylie-Rosett J; American Heart Association Statistics Committee and Stroke Statistics Subcommittee. Executive summary: heart disease and stroke statistics--2010 update: a report from the American Heart Association. *Circulation*. 2010; 121:948-954.
3. Li M, Zhou T, Yang LF, Peng ZH, Ding J, Sun G. Diagnostic accuracy of myocardial magnetic resonance perfusion to diagnose ischemic stenosis with fractional flow reserve as reference: systematic review and meta-analysis. *JACC Cardiovasc Imaging*. 2014; 7:1098-1105.

4. Zhou T, Yang LF, Zhai JL, Li J, Wang QM, Zhang RJ, Wang S, Peng ZH, Li M, Sun G. SPECT myocardial perfusion versus fractional flow reserve for evaluation of functional ischemia: a meta analysis. *Eur J Radiol.* 2014; 83:951-956.
5. Takx RA, Blomberg BA, El Aidi H, Habets J, de Jong PA, Nagel E, Hoffmann U, Leiner T. Diagnostic accuracy of stress myocardial perfusion imaging compared to invasive coronary angiography with fractional flow reserve meta-analysis. *Circ Cardiovasc Imaging.* 2015; 8. pii: e002666.
6. Desai RR, Jha S. Diagnostic performance of cardiac stress perfusion MRI in the detection of coronary artery disease using fractional flow reserve as the reference standard: a meta-analysis. *AJR Am J Roentgenol.* 2013; 201:W245-252.
7. Bettencourt N, Chiribiri A, Schuster A, Ferreira N, Sampaio F, Pires-Morais G, Santos L, Melica B, Rodrigues A, Braga P, Azevedo L, Teixeira M, Leite-Moreira A, Silva-Cardoso J, Nagel E, Gama V. Direct comparison of cardiac magnetic resonance and multidetector computed tomography stress-rest perfusion imaging for detection of coronary artery disease. *J Am Coll Cardiol.* 2013; 61:1099-1107.
8. Kamiya K, Sakakibara M, Asakawa N, Yamada S, Yoshitani T, Iwano H, Komatsu H, Naya M, Chiba S, Yamada S, Manabe O, Kikuchi Y, Oyama-Manabe N, Oba K, Tsutsui H. Cardiac magnetic resonance performs better in the detection of functionally significant coronary artery stenosis compared to single-photon emission computed tomography and dobutamine stress echocardiography. *Circ J.* 2014; 78:2468-2476.
9. Jaarsma C, Leiner T, Bekkers SC, Crijs HJ, Wildberger JE, Nagel E, Nelemans PJ, Schalla S. Diagnostic performance of noninvasive myocardial perfusion imaging using single-photon emission computed tomography, cardiac magnetic resonance, and positron emission tomography imaging for the detection of

- obstructive coronary artery disease: a meta-analysis. *J Am Coll Cardiol.* 2012; 59:1719-1728.
10. Bossuyt PM, Reitsma JB, Bruns DE, Gatsonis CA, Glasziou PP, Irwig LM, Lijmer JG, Moher D, Rennie D, de Vet HC; Standards for Reporting of Diagnostic Accuracy. Towards complete and accurate reporting of studies of diagnostic accuracy: the STARD initiative. *BMJ* 2003; 326:41-44.
 11. Whiting PF, Rutjes AW, Westwood ME, Mallett S, Deeks JJ, Reitsma JB, Leeflang MM, Sterne JA, Bossuyt PM; QUADAS-2 Group. QUADAS-2: a revised tool for the quality assessment of diagnostic accuracy studies. *Ann Intern Med.* 2011; 155:529-536.
 12. Cury RC, Nieman K, Shapiro MD, Butler J, Nomura CH, Ferencik M, Hoffmann U, Abbara S, Jassal DS, Yasuda T, Gold HK, Jang IK, Brady TJ. Comprehensive assessment of myocardial perfusion defects, regional wall motion, and left ventricular function by using 64-section multidetector CT. *Radiology* 2008; 248:466-475
 13. Baumann S, Wang R, Schoepf UJ, Steinberg DH, Spearman JV, Bayer RR 2nd, Hamm CW, Renker M. Coronary CT angiography-derived fractional flow reserve correlated with invasive fractional flow reserve measurements--initial experience with a novel physician-driven algorithm. *Eur Radiol.* 2015; 25:1201-1207.
 14. Vignon-Clementel IE, Figueroa CA, Jansen KE, Taylor CA. Outflow boundary conditions for 3D simulations of non-periodic blood flow and pressure fields in deformable arteries. *Comput Methods Biomech Biomed Engin* 2010; 13:625–640.
 15. Abidov A, Hachamovitch R, Hayes SW, Friedman JD, Cohen I, Kang X, De Yang L, Thomson L, Germano G, Slomka P, Berman DS. Are shades of gray prognostically seful in reporting myocardial perfusion single-photon emission

- computed tomography? *Circ Cardiovasc Imaging* 2009; 2:290–298.
16. Reitsma J, Glas A, Rutjes A, Scholten R, Bossuyt P, Zwinderman A. Bivariate Analysis of Sensitivity and Specificity Produces Informative Summary Measures in Diagnostic Reviews." *Journal of Clinical Epidemiology*. 2005;58:982-990.
17. Dwamena BA, Sylvester R, Carlos RC. midas: meta-analysis of diagnostic accuracy studies[EB/OL]. <http://fmwww.bc.edu/repec/bocode/m/midas.pdf>
18. Riley RD, Abrams KR, Lambert PC, Sutton AJ, Thompson JR. An evaluation of bivariate random-effects meta-analysis for the joint synthesis of two correlated outcomes. *Stat Med*. 2007; 26:78-97.
19. Riley RD, Abrams KR, Sutton AJ, Lambert PC, Thompson JR. Bivariate random-effects meta-analysis and the estimation of between-study correlation. *BMC Med Res Methodol*. 2007; 7:3.
20. Deeks JJ, Macaskill P, Irwig L. The performance of tests of publication bias and other sample size effects in systematic reviews of diagnostic test accuracy was assessed. *J Clin Epidemiol*. 2005; 58:882-893.
21. Schwitter J, Wacker CM, Wilke N, Al-Saadi N, Sauer E, Huettle K, Schönberg SO, Debl K, Strohm O, Ahlstrom H, Dill T, Hoebel N, Simor T; MR-IMPACT investigators. Superior diagnostic performance of perfusion-cardiovascular magnetic resonance versus SPECT to detect coronary artery disease: The secondary endpoints of the multicenter multivendor MR-IMPACT II (Magnetic Resonance Imaging for Myocardial Perfusion Assessment in Coronary Artery Disease Trial). *J Cardiovasc Magn Reson*. 2012; 14:61.
22. Greenwood JP, Motwani M, Maredia N, Brown JM, Everett CC, Nixon J, Bijsterveld P, Dickinson CJ, Ball SG, Plein S. Comparison of Cardiovascular Magnetic Resonance and Single-Photon Emission Computed Tomography

- in Women With Suspected Coronary Artery Disease From the Clinical Evaluation of Magnetic Resonance Imaging in Coronary Heart Disease (CE-MARC) Trial. *Circulation*. 2014; 129:1129-1138.
23. Hamon M, Fau G, Née G, Ehtisham J, Morello R, Hamon M. Meta-analysis of the diagnostic performance of stress perfusion cardiovascular magnetic resonance for detection of coronary artery disease. *J Cardiovasc Magn Reson* 2010; 12:29.
 24. Wagner A, Mahrholdt H, Holly TA, Elliott MD, Regenfus M, Parker M, Klocke FJ, Bonow RO, Kim RJ, Judd RM. Contrast-enhanced MRI and routine single photon emission computed tomography (SPECT) perfusion imaging for detection of subendocardial myocardial infarcts: an imaging study. *Lancet* 2003; 361:374–379.
 25. Klein C, Nekolla SG, Bengel FM, Momose M, Sammer A, Haas F, Schnackenburg B, Delius W, Mudra H, Wolfram D, Schwaiger M. Assessment of myocardial viability with contrast-enhanced magnetic resonance imaging: comparison with positron emission tomography. *Circulation* 2002; 105:162–167.
 26. Hajjiri MM, Leavitt MB, Zheng H, Spooner AE, Fischman AJ, Gewirtz H. Comparison of positron emission tomography measurement of adenosine-stimulated absolute myocardial blood flow versus relative myocardial tracer content for physiological assessment of coronary artery stenosis severity and location. *JACC Cardiovasc Imaging*. 2009; 2:751–758.
 27. Muzik O, Duvernoy C, Beanlands RS, Sawada S, Dayanikli F, Wolfe ER Jr, Schwaiger M. Assessment of diagnostic performance of quantitative flow measurements in normal subjects and patients with angiographically documented coronary artery disease by means of nitrogen-13 ammonia and positron emission tomography. *J Am Coll Cardiol*. 1998; 31:534–540
 28. Dai N, Xia HH, Xu YW. Noninvasive approach to assess coronary artery stenoses

- and ischemia. JAMA. 2013; 309:235-236.
29. Ho KT, Chua KC, Klotz E, Panknin C. Stress and rest dynamic myocardial perfusion imaging by evaluation of complete time-attenuation curves with dual-source CT. JACC Cardiovasc Imaging 2010;3:811 –820.
 30. George RT, Arbab-Zadeh A, Miller JM, Vavere AL, Bengel FM, Lardo AC, Lima JA. Computed tomography myocardial perfusion imaging with 320-row detector computed tomography accurately detects myocardial ischemia in patients with obstructive coronary artery disease. Circ Cardiovasc Imaging 2012;5:333–340
 31. George RT, Mehra VC, Chen MY, Kitagawa K, Arbab-Zadeh A, Miller JM, Matheson MB, Vavere AL, Kofoed KF, Rochitte CE, Dewey M, Yaw TS, Niinuma H, Brenner W, Cox C, Clouse ME, Lima JA, Di Carli M. Myocardial CT perfusion imaging and SPECT for the diagnosis of coronary artery disease: a head-to-head comparison from the CORE320 multicenter diagnostic performance study. Radiology. 2014; 272:407-416.
 32. Pijls NH, van Schaardenburgh P, Manoharan G, Boersma E, Bech JW, van't Veer M et al. Percutaneous Coronary Intervention of Functionally Nonsignificant Stenosis: 5-Year Follow-Up of the DEFER Study. J Am Coll Cardiol 2007; 49: 2105 -2111.
 33. Pijls NH, Fearon WF, Tonino PA, Siebert U, Ikeno F, Bornschein B, van't Veer M, Klauss V, Manoharan G, Engstrøm T, Oldroyd KG, Ver Lee PN, MacCarthy PA, De Bruyne B; FAME Study Investigators. Fractional flow reserve versus angiography for guiding percutaneous coronary intervention in patients with multivessel coronary artery disease: 2-year follow-up of the FAME (Fractional Flow Reserve Versus Angiography for Multivessel Evaluation) study. J Am Coll Cardiol 2010; 56:177-184

34. De Bruyne B, Pijls NH, Kalesan B, Barbato E, Tonino PA, Piroth Z, Jagic N, Möbius-Winkler S, Rioufol G, Witt N, Kala P, MacCarthy P, Engström T, Oldroyd KG, Mavromatis K, Manoharan G, Verlee P, Frobert O, Curzen N, Johnson JB, Jüni P, Fearon WF; FAME 2 Trial Investigators. Fractional flow reserve-guided PCI versus medical therapy in stable coronary disease. *N Eng J Med* 2012; 367:991-1001.
35. Pijls NH, De Bruyne B, Peels K, Van Der Voort PH, Bonnier HJ, Bartunek J, Koolen JJ, Koolen JJ. Measurement of fractional flow reserve to assess the functional severity of coronary-artery stenoses. *N Engl J Med* 1996; 334:1703 – 1709
36. Plein S, Motwani M. Fractional flow reserve as the reference standard for myocardial perfusion studies: fool's gold? *Eur Heart J Cardiovasc Imaging*. 2013; 14:1211-1213.
37. Ramanna N. Fractional flow reserve is a useful reference standard for myocardial perfusion studies with limitations. *Eur Heart J Cardiovasc Imaging*. 2014; 15:473-474.

Figure legends:**Figure 1. Flow Chart of Literature Search**

Of 530 potentially relevant citations, 74 articles met our inclusion criteria and were included for final analysis.

CAD: coronary artery disease; CFR: coronary flow reserve; CMR: cardiac magnetic resonance; CTP: computed tomographic perfusion imaging; DSE: dobutamine stress echocardiography; FFR: fractional flow reserve; FFR_{CT}: fractional flow reserve derived from Computed Tomography; FN: false negative; FP: false positive; PET: positron emission tomography; SPECT: single-photon emission computed tomography; TN: true negative; TP: true positive

Figure 2. Pooled sensitivity and specificity estimates for FFR_{CT}, CMR, PET, CTP, SPECT and DSE on patient- and vessel-based analyses

The pooled sensitivity and specificity of 6 non-invasive cardiac imaging modalities in all the patients with known or suspected coronary artery disease on both per-patient and per-vessel analyses.

CMR: cardiac magnetic resonance; CTP: computed tomographic perfusion imaging;

DSE: dobutamine stress echocardiography; FFR_{CT}: fractional flow reserve derived

from Computed Tomography; PET: positron emission tomography; SPECT:

single-photon emission computed tomography.

* indicates $P < 0.05$ when compared with FFR_{CT}, ** indicates $P < 0.01$ when compared with FFR_{CT}

indicates $P < 0.05$ when compared with CMR, ## indicates $P < 0.01$ when compared with CMR

& indicates $P < 0.05$ when compared with PET, && indicates $P < 0.01$ when compared with PET

\$ indicates $P < 0.05$ when compared with CTP, \$\$ indicates $P < 0.01$ when compared with CTP

Figure 3. CMR, CTP, PET, FFR_{CT}, DSE and SPECT for detecting CAD on vessel- and patient-based analysis

Fitted SROC (summary receiver-operating characteristics) curves for direct comparison of the diagnostic performance of positron emission tomography (PET); cardiac magnetic resonance (CMR); computed tomographic perfusion imaging (CTP); Fractional flow reserve derived from Computed Tomography (FFR_{CT}), single-photon emission computed tomography (SPECT) and dobutamine stress echocardiography (DSE) for the detection of functional coronary artery disease (CAD) on a vessel-based level (A) and patient-based(B) level: Each dot represents a single study. The area under the curve (AUC) reflects the overall diagnostic performance and is expressed as a value between 0 and 1, with higher values indicating better test performance. On per-vessel analysis (A), the AUCs were 0.94, 0.94, 0.92, 0.89, 0.86 and 0.83 for CMR (black line), CTP (green line), PET (blue line), FFR_{CT} (red line), DSE (yellow line) and SPECT (purple line), respectively; on per-patient analysis (B), the AUCs were 0.94, 0.92, 0.91, 0.90, 0.85 and 0.78 for CTP (green line), PET (blue line), CMR (black line), FFR_{CT} (red line), SPECT (purple line) and DSE (yellow line), respectively.

Figure 4. Effects of different imaging evaluation methods on the pooled sensitivity and specificity of CMR, CTP and PET on coronary territory and patient basis analysis

Comparison of the pooled sensitivity and specificity estimates when different analysis methods applied in CMR, CTP and PET on coronary territory and patient basis analysis: PD, MBF and MPRI were applied for CMR imaging analysis; PD and MBF were applied for CTP imaging analysis; CFR and MBF were applied for PET imaging analysis

CFR: coronary flow reserve; CMR: cardiac magnetic resonance; CTP: computed tomographic perfusion imaging; PD: perfusion defect; PET: positron emission tomography; MBF: myocardial blood flow; MPRI: myocardial perfusion index

* indicates the value significantly lower than that of PD

indicates the value significantly lower than that of MBF

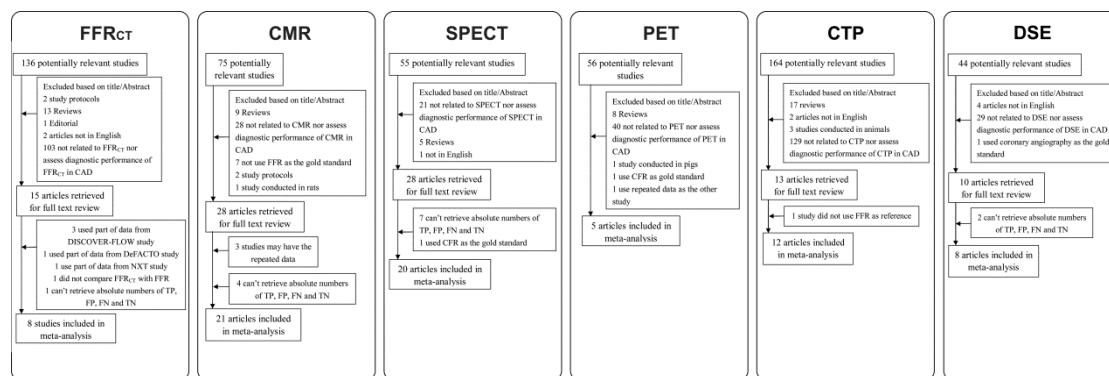


Figure 1

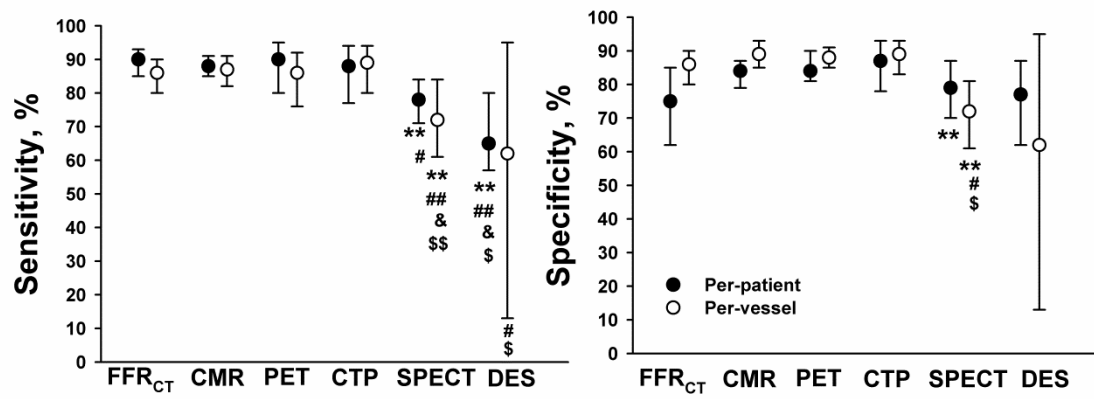


Figure 2

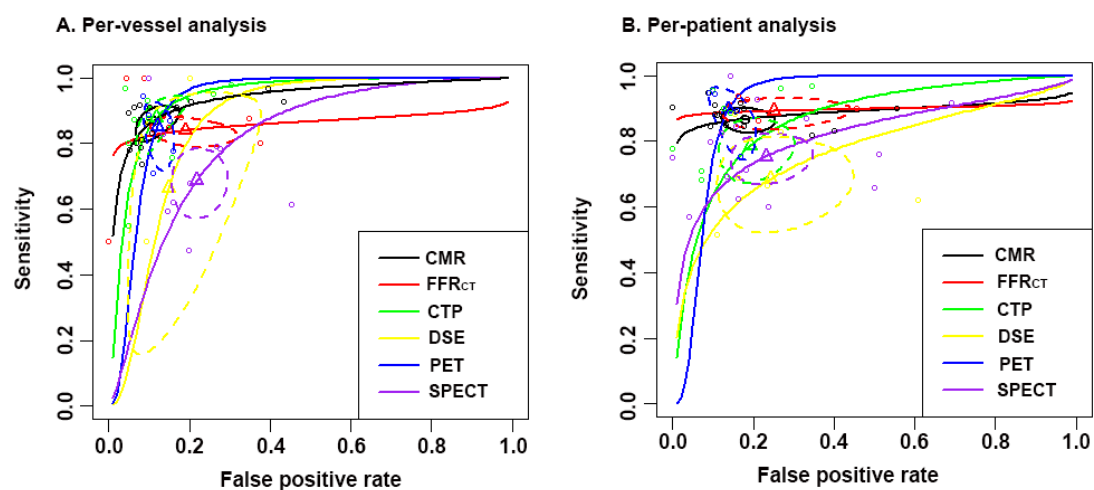


Figure 3

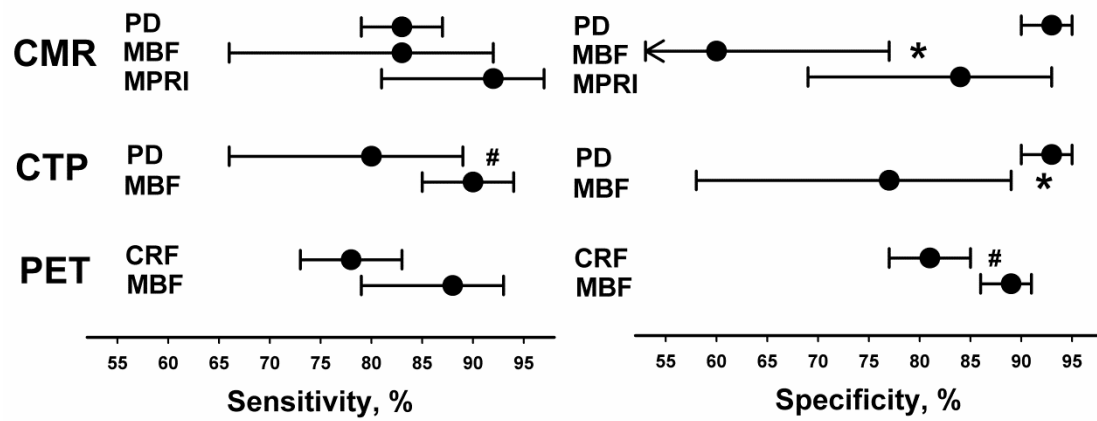


Figure 4

Table 1. Characteristics of included studies

Source	Populations	Mean Age \pm SD, y	Study Size	Male	Prevalence of CAD	Approach used for primary analysis	Proportion of abnormal FFR	Cut-off value for CAD on FFR
FFR_{CT}								
Wang et al, 2015	Suspected CAD	58 \pm 12	32	66%	NA	Model by Siemens	25%	0.80
Coenen et al, 2014	Suspected or known CAD	61.4 \pm 9.2	106	77%	42.3%	Model by Siemens	25%	0.80
Renker et al, 2014	Suspected or known CAD	61.2 \pm 12.0	53	64%	31%	Model by Siemens	30%	0.80
Kim et al, 2013	Known CAD	65.0 \pm 9.1	44	80%	100%	Model by Heart flow	3.5%	0.80
Nørgaard et al, 2013	Suspected or known CAD	64.0 \pm 10.0	254	64%	NA	Model by Heart flow	32%	0.80
Zhang et al, 2013	Known CAD	NA	7	NA	100%	Model by Zhang et al	29%	0.80
Min et al, 2012	Suspected CAD	62.9 \pm 8.7	252	70.60%	46.50%	Model by Heart flow	37.1%	0.80
Koo et al, 2011	Suspected or known CAD	62.7 \pm 8.5	103	72%	NA	Model by Heart flow	36.5%	0.80
CMR								
Manka et al, 2015	Suspected CAD	62.9 \pm 10	155	70%	NA	PD, MIB	56.7%	0.80
Pan et al, 2015	Suspected or known CAD	60.1 \pm 6.4	71	80%	54.9%	TPG, TPGR	25.8%	0.75
Kamiya et al, 2014	known CAD	67.5 \pm 7.2	25	56%	100%	PD	38%	0.80
Ponte et al, 2014	Suspected CAD	62 \pm 8.1	95	68%	43%	PD	NA	0.80
Ebersberger et al, 2013	Suspected or known CAD	63 \pm 14	116	61%	78%	PD	27%	0.80
Chiribiri et al, 2013	Suspected or known	59 \pm 11	30	73%	22%-29%	PD, TPG	17.8%	0.80

CAD								
Groothuis et al, 2013	Suspected CAD	56±10	88	NA	26%	PD	NA	0.75
Bettencourt et al, 2012	Suspected CAD	62±8	103	66%	42%	PD	24.3%	0.80
Jogiya et al, 2012	Suspected or known CAD	63.5±10.8	53	64%	64%	PD	29.6%	0.75
Manka et al, 2012	Suspected or known CAD	63.7±11.9	120	75%	58%	PD	NA	0.75
Bernhardt et al, 2012	Suspected or known CAD	62.0 ± 10.9	34	76.5%	NA	MPRI	NA	0.80
Huber et al, 2012	suspected CAD	67±12.3	31	87%	74%	MPRI, MBF relative BOLD signal intensity increase	47.8%	0.75
Walcher et al, 2012	suspected CAD	63.1±9.9	36	75%	NA	MPRI, MBF relative BOLD signal intensity increase	NA	0.80
Lockie et al, 2011	Suspected or known CAD	57.4±9.6	42	79%	NA	MBF	26.3%	0.75
Kirschbaum et al, 2010	Suspected CAD	64±10	50	76%	NA	MPRI	42.7%	0.80
Watkins et al, 2009	Suspected or known CAD	60±9	103	73%	NA	PD	40.3%	0.75
Costa et al, 2007	Suspected CAD	65±11	37	43%	NA	MBF	31.8%	0.75
Futamatsu et al, 2007	Suspected or known CAD	65±11	37	43%	NA	MPRI	NA	0.75
Kühl et al, 2007	Suspected or known CAD	64±13	19	68%	NA	MPRI	23.5%	0.75
Rieber et al, 2006	known or suspected CAD	65.5±8.1	43	88%	67%	MPRI	11.6%	0.75

PET

Danad et al, 2014	Suspected CAD	61±9	281	68%	NA	MBF, CRF	21.4%	0.80
Danad et al, 2014	known CAD	59±10	66	67%	100%	MBF, CRF	26.5%	0.80
Joutsiniemi et al, 2014	Suspected CAD	64	104	38%	45%	MBF, CRF	25.6%	0.80
Danad et al, 2013	Suspected or known CAD	61±10	120	64%	41%	MBF, Relative Uptake	25.8%	0.80
Kajander et al, 2011	Suspected CAD	NA	104	NA	37%	MBF	23.7%	0.80
SPECT								
Kamiya et al, 2014	known CAD	67.5±7.2	25	56%	100%	SDSr	43.7%	0.80
Pirich et al, 2014	Suspected CAD	69 ±11	97	63%	41%	SDSr	NA	0.80
Mouden et al, 2013	Suspected or known CAD	66±11	100	64%	NA	SSSr+SRSr	NA	0.75
Schaap et al, 2013	Suspected CAD	62.5±10.1	98	68%	57%	SSSr	38.4	0.80
Jakljevic et al, 2012	Suspected CAD	66±10	103	79%	NA	SDSr	NA	0.80
Sahiner et al, 2012	Suspected or known CAD	NA	58	67%	NA	SSS+SDS, SSS, PD	NA	0.75
Schaap et al, 2012	Suspected CAD	62.7±9.7	129	65%	50%	SSS	NA	0.80
Melikian et al, 2010	Known CAD	64±10	67	63%	100%	SDSr+SR Sr	39.8%	0.80
Förster et al, 2010	Known CAD	67±8.5	72	61%	100%	SDSr+SR Sr, SDSr	46.3%	0.75
Ragosta et al, 2007	Known CAD	62±11	36	75%	100%	SDSr	61.4%	0.75
Hacker et al, 2005	Suspected or known CAD	NA	50	NA	100%	SDSr, SSSr,	NA	0.75
Erhard et al, 2005	Known CAD	64.4±9.7	47	62%	100%	SDSr	NA	0.75
Morishi	Suspected	66±8	20	80%	40%	SDSr	NA	0.75

ma et al, 2004	d CAD							
Rieber et al, 2004	Suspected CAD	64±10	48	60%	100%	SDSr	NA	0.75
Yanagisawa et al, 2002	Suspected CAD	61 ±9	165	84%	100%	SSSr	52.9%	0.75
Bruyne et al, 2001	Known CAD	61±11	57	77%	100%	SDSr	41.2%	0.75
Seo et al, 2002	Known CAD	56±13	25	76%	100%	SDS	NA	0.75
Caymaz et al, 2000	Known CAD	53.3±10.2	30	67%	NA	SSSr	50%	0.75
Pijls et al, 1996	Known CAD	54±8	45	62%	NA	SSSr	NA	0.75
Tron et al, 1995	Suspected or known CAD	56±13	62	89%	100%	SDSr	55.7%	0.75
CTP								
Yang et al, 2015	Suspected CAD	64.0±9.6	75	77%	NA	PD, WMA myocardial enhancement ratio	41%	
Habis et al, 2015	Suspected CAD	65±12	32	81%	100%		55.6%	
Kono et al, 2014	Suspected or known CAD	62.3±8.7	42	81%	NA	MBF, CFR	49.5%	0.80
Bettencourt et al, 2013	Suspected CAD	62±8.0	105	67%	46%	PD	NA	0.80
Rossi et al, 2013	Suspected or known CAD	60±10	80	79%	50%	MBF	26.7%	0.75
Huber et al, 2013	Suspected CAD	NA	32	NA	63%	Time to peak, area under the curve, Upslope, Peak enhancement, MBF	NA	0.75
Greif et al, 2013	Suspected or known CAD	70.4±9	65	65%	NA	MBF	20.5%	0.80
Choo et al, 2013	Suspected CAD	61.7 ± 20.5	37	76%	NA	PD	35.8%	0.75

Bettencourt et al, 2013	Suspected CAD	62 ± 8.0	101	67%	44%	PD	24.1%	0.80
Ko et al, 2012	Suspected CAD	62.1±9.9	28	67.5%	NA	TPG, PD	33.1%	0.80
Bamberg et al, 2011	Suspected or known CAD	68.1±10	33	76%	NA	MBF	35.4%	0.75
Ko et al, 2011	Suspected CAD	65.1 ± 8.3	42	64.7%	NA	PD	47.7%	0.80
DSE								
Pattanshetty et al, 2015	Suspected or known CAD	61 ± 10	96	48%	43%	WMA	NA	0.80
Utsunomiya et al, 2015	Known CAD	69 ± 8	110	75%	100%	WMA,	NA	0.80
Kamiya et al, 2014	Known CAD	67.5±7.2	25	56%	NA	WMA	39.4%	0.80
Jung et al, 2008	Known CAD	65±10	70	64%	100%	WMA	NA	0.75
Weidemann et al, 2007	Known CAD	NA	30	NA	100%	WMA	NA	0.75
Erhard et al, 2005	Known CAD	64.4±9.7	47	61.7%	100%	WMA	NA	0.76
Riber et al, 2004	Suspected CAD	64±10	48	60%	100%	WMA	NA	0.75
Manuel et al, 2001	Known CAD	NA	21	NA	100%	WMA	13%	0.75

CAD: coronary artery disease; CMR: cardiac magnetic resonance; CTP: computed tomographic perfusion imaging; CRF: Coronary flow reserve; FFR: fractional flow reserve; FFR_{CT}: fractional flow reserve derived from Computed Tomography; MBF: Myocardial blood flow; MIB: Myocardial ischemic burden; MPRI: Myocardial perfusion reserve index; NA: not available; PD: perfusion defect; PET: positron emission tomography; SD: standard deviation; SDS: summed difference score; SDSr: regional summed difference score; SPECT: single-photon emission computed tomography; SSS: Summed stress score; SSSr: regional summed stress score; TPG: transmural perfusion gradient; TPGR: transmural perfusion gradient reserve; WMA: wall motion abnormality

Table 2. Pooled sensitivity, specificity, PLR, NLR, DOR and AUROC for CMR, FFR_{CT}, CTP, DSE, PET and SPECT by bivariate analysis on both coronary territory and patient basis

Imag ing test	N of stu dy	N of subje cts	Parameters					
			Sen%(95% CI)	Spe%(95% CI)	PLR(95% CI)	NLR(95 % CI)	DOR(95% CI)	AUROC(95% CI)
Coronary territory basis								
CMR	15	3260	87(82-9 1)	89(85-9 3)	8.15(5.76, 11.53)	0.14(0.10, 0.20)	57.93(38.31, 87.61)	0.94(0.92, 0.96)
FFR _C T	8	2782	86(80-9 0)	83(73-9 0)	5.10(3.00, 8.65)	0.17(0.12, 0.25)	29.37(12.91, 66.80)	0.89(0.86, 0.91)
CTP	10	1444	89(80-9 4)	89(83-9 3)	7.82(5.48, 11.17)	0.13(0.07, 0.23)	61.98(37.81, 101.60)	0.94(0.92, 0.96)
DES	2	94	62(13-9 5)	87(73-9 4)	4.66(1.74, 12.47)	0.44(0.11, 1.85)	10.51(1.10,1 00.09)	0.86(0.82, 0.88)
PET	5	2017	86(76-9 2)	88(85-9 1)	7.15(5.46, 9.35)	0.17(0.10, 0.29)	43.39(21.04, 89.49)	0.92(0.89, 0.94)
SPEC T	9	1288	72(61-8 1)	79(73-8 4)	3.45(2.53, 4.72)	0.36(0.24, 0.52)	9.71(5.14,18. 36)	0.83(0.79, 0.86)
Patient basis								
CMR	15	1054	88(85-9 1)	84(79-8 7)	5.62(4.08, 7.73)	0.14(0.11, 0.18)	40.69(24.92, 66.46)	0.91(0.88, 0.93)
FFR _C T	4	662	90(85-9 3)	75(62-8 5)	3.60(2.26, 5.72)	0.14(0.09, 0.21)	25.87(12.27, 54.55)	0.90(0.87, 0.92)
CTP	8	532	88(77-9 4)	87(78-9 3)	6.97(4.17, 11.67)	0.14(0.08, 0.26)	49.88(27.02, 92.08)	0.94(0.91, 0.96)
DES	6	359	69(57-8 0)	77(62-8 7)	2.96(1.69, 5.16)	0.40(0.27, 0.60)	7.40(3.11,17. 62)	0.78(0.74, 0.82)
PET	4	609	90(80-9 5)	84(81-9 0)	6.60(4.57, 9.53)	0.12(0.06, 0.24)	56.59(20.28, 157.87)	0.92(0.89, 0.94)
SPEC T	15	1142	78(71-8 4)	79(70-8 7)	3.76(2.52, 5.63)	0.28(0.21, 0.37)	13.52(7.53,2 4.30)	0.85(0.81, 0.88)

AUROC=Area under summary Receiver Operating Characteristic; CI: confidence interval; CMR: cardiac magnetic resonance; CTP: computed tomographic perfusion imaging; DOR=Diagnostic Odds Ratio; FFR_{CT}: fractional flow reserve derived from Computed Tomography; NLR: Negative Likelihood Ratio; PET: positron emission tomography; PLR: Positive Likelihood Ratio; Sen: Sensitivity; Spe: Specificity; SPECT: single-photon emission computed tomography

Table 3. Pooled estimates when different imaging evaluation methods applied in CMR, CTP and PET on both coronary territory and patient basis using bivariate Analysis

Methods	subgroup	N of study	N of subjects	Parameters					
				Sen	Spe	PLR	NLR	DOR	AUROC
Coronary territory basis									
CMR	PD	10	2115	83(79-87)	93(90-95)	11.29(8.42-15.13)	18(14-23)	62.60(426-97.34)	0.94(0.92-0.96)
	MBF	3	193	83(66-92)	60(40-77)	4.06(1.92-8.62)	22(11-43)	18.58(6.91-49.94)	0.88(0.85-0.90)
	MPRI	4	278	92(81-97)	84(69-93)	5.91(2.86-12.18)	09(04-22)	65.71(22.68-1934)	0.95(0.93-0.97)
CTP	PD	5	798	80(66-89)	93(90-95)	11.53(8.13-16.37)	22(13-38)	52.77(27.24-102.21)	0.95(0.92-0.96)
	MBF	4	592	90(85-94)	77(58-89)	3.98(1.97- 8.01)	13(08-20)	31.90(11.87-85.74)	0.91(0.88-0.93)
PET	CRF	4	1075	78(73-83)	81(77-85)	4.15(3.21-5.35)	27(21-34)	15.60(9.69-25.09)	0.86(0.83-0.89)
	MBF	6	2329	88(79-93)	89(86-91)	7.73(5.90-113)	14(08-24)	55.14(25.61-118.73)	0.93(0.90-0.95)
Patient basis									
CMR	PD	10	891	89(86-91)	87(83-90)	6.70(5.27-8.51)	13(10-17)	51.82(34.66-77.45)	0.94(0.92-0.96)
	MBF	1	37	83(52-96)	60(40-77)	2.08(1.21-3.59)	28(08-1.02)	7.50(1.35-41.72)	0.80(0.76-0.83)
	MPRI	4	124	81(63-91)	76(47-92)	3.40(1.24-9.33)	25(11-57)	14.49(2.57-767)	0.85(0.82-0.88)
CTP	PD	5	177	83(69-91)	89(80-94)	7.45(2.45-13.06)	20(11-36)	38.00(18.65-77.40)	0.93(0.90-0.95)
	MBF	3	355	91(75-97)	89(59-98)	8.54(1.89-38.51)	11(04-27)	81.48(21.02-315.83)	0.95(0.93-0.97)
PET	CRF	3	713	84(77-90)	75(61-85)	3.36(2.00-5.66)	21(12-36)	16.18(5.87-44.61)	0.88(0.85-0.90)
	MBF	5	505	91(83-96)	87(81-93)	7.16(5.03-121)	10(05-20)	711(26.59-184.87)	0.93(0.91-0.95)

AUROC=Area under summary Receiver Operating Characteristic; CMR: cardiac magnetic resonance; CTP: computed tomographic perfusion imaging; CRF: Coronary flow reserve; DOR: Diagnostic Odds Ratio; MBF: Myocardial blood flow; MPRI: Myocardial perfusion reserve index; NLR: Negative Likelihood Ratio; PD: perfusion defect; PET: positron emission tomography; PLR: Positive Likelihood Ratio; Sen: Sensitivity; Spe: Specificity

Table 4. Effects of different imaging evaluation methods on the pooled sensitivity and specificity of CMR, CTP and PET on coronary territory and patient basis analysis

Imaging modalities	Subgroup comparisons	Coronary territory basis				Patient basis			
		Sen		Spe		Sen		Spe	
		F value	P value	F value	P value	F value	P value	F value	P value
CMR	PD vs. MBF	0.23	0.63	5.28	0.02	-	-	-	-
	PD vs. MPRI	2.48	0.11	3.45	0.06	-	-	-	-
	MBF vs. MPRI	2.60	0.10	0.28	0.59	-	-	-	-
CTP	PD vs. MBF	3.92	0.04	5.46	0.02	1.16	0.28	0.27	0.60
			8		0		2		6
PET	CRF vs. MBF	2.15	0.14	7.97	0.00	1.04	0.30	7.03	0.00
			3		5		7		8

CMR: cardiac magnetic resonance; CTP: computed tomographic perfusion imaging; CRF: Coronary flow reserve; DOR: Diagnostic Odds Ratio; MBF: Myocardial blood flow; MPRI: Myocardial perfusion reserve index; PD: perfusion defect; PET: positron emission tomography; Sen: Sensitivity; Spe: Specificity

“-” means comparison cannot be conducted because of the limited studies

P<0.05 indicates significance